

An explanatory model to validate the way water activity rules periodic terrace generation in *Proteus mirabilis* swarm

Emmanuel Frénod ^{*} Olivier Sire [†]

October 27, 2018

Abstract - This paper explains the biophysical principles which, according to us, govern the *Proteus mirabilis* swarm phenomenon. Then, this explanation is translated into a mathematical model, essentially based on partial differential equations. This model is then implemented using numerical methods of the finite volume type in order to make simulations. The simulations show most of the characteristics which are observed *in situ* and in particular the terrace generation.

Keywords - *Proteus mirabilis* swarm, modelling, partial differential equations, finite volumes.

Contents

1	Introduction	1
2	Explanation of the principles governing the swarm	4
3	Translation of the principles into a model	5
4	Implementation	9
5	Simulations	12
5.1	Simulation 1	13
5.2	Simulation 2	14
5.3	Simulation 3	19
6	Conclusion	21

1 Introduction

Proteus mirabilis is a pathogenic bacterium of the urinary tract. Under specific conditions, within a *Proteus mirabilis* colony grown on a solid substratum, some bacteria, the standard form of which is a short cell, called “swimmer” or “vegetative”, undergo differentiation into elongated cells, called “swarmer” cells, capable of translocation. Having this translocation ability, those swarmer cells may begin to colonize the surrounding medium. After a given period of time, the swarm phenomenon stops and the swarmer cells de-differentiate to produce vegetative cells which would, later on, be able to differentiate again and resume colonization.

^{*}Université Européenne de Bretagne, Lab-STICC (UMR CNRS 3192), Université de Bretagne-Sud, Centre Yves Coppens, Campus de Tohannic, F-56017, Vannes

[†]Université Européenne de Bretagne, LIMATB, Université de Bretagne-Sud, Centre Yves Coppens, Campus de Tohannic, F-56017, Vannes

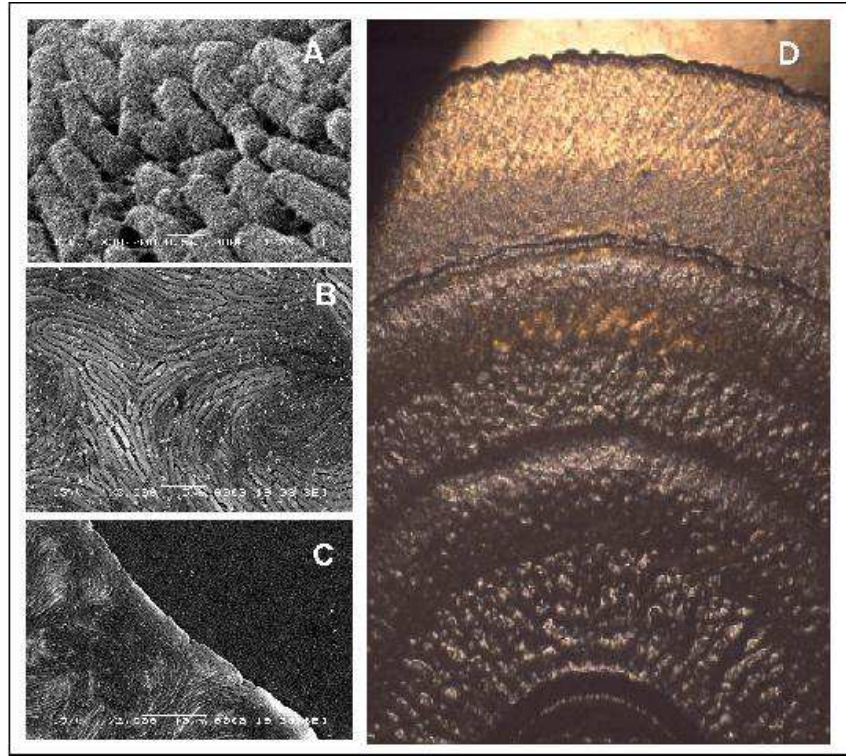


Figure 1: *Proteus mirabilis*: Short vegetative cells (A); swarmer cells (B); periphery of a colony (C) and a swarm colony with terraces (D). Scales : (A): bar = $0.5 \mu\text{m}$; (B): bar = $5 \mu\text{m}$; (C): bar = $10 \mu\text{m}$ and (D): colony radius = 3 cm .

This swarm phenomenon is illustrated in Figures 1 and 2. In Figure 1, the *Proteus mirabilis* cells can be seen in their standard vegetative forms (A). They are about $2 \mu\text{m}$ long. The elongated swarmer cells which range between 10 to $25 \mu\text{m}$ and which are covered by hundreds of flagella can also be seen (B). The third panel (C) displays a close up of the peripheral edge of a bacterial colony on an agar medium filling a Petri dish. The area around the edge is the theater of fast motion of swarmer cell flagella making it moves while the medium is gradually colonized. The last panel (D) shows a colony after several hours of swarming. It forms a thin film showing the specific pattern: concentric rings called terraces. Those rings are made by variations in the colony's thickness.

Figure 2 which displays three snapshots of the colony expansion on agar during an active migration phase. The expansion process is clearly seen from the progression of the colony's edge. The central inoculum is located in the bottom right of each picture.

For a precise and synthetic description of *Proteus mirabilis* swarm phenomenon, we refer to Rauprich *et al.* [38] and Matsuyama *et al.* [33]. Among all aspects described in those references, periodic alternation of swarm phases and of consolidation phases, without any motion, seem to be the most typical one. This alternation gives rise to terraces as a resulting effect. The second one concerns the cell size distribution and was pointed out in Matsuyama *et al.* [33]. As for space distribution at a given time, the swarming front is essentially constituted by long cells and the proportion of shorter cells grows while moving towards the colony interior. Concerning time distribution at a given place, the colonization starts with long hyperflagellated cells and then the proportion of shorter cells grows. The third typical fact, pointed out in Lahaye *et al.* [24, 25] is that the consolidation phase begins even though swarmer cells are still present in the colony front.

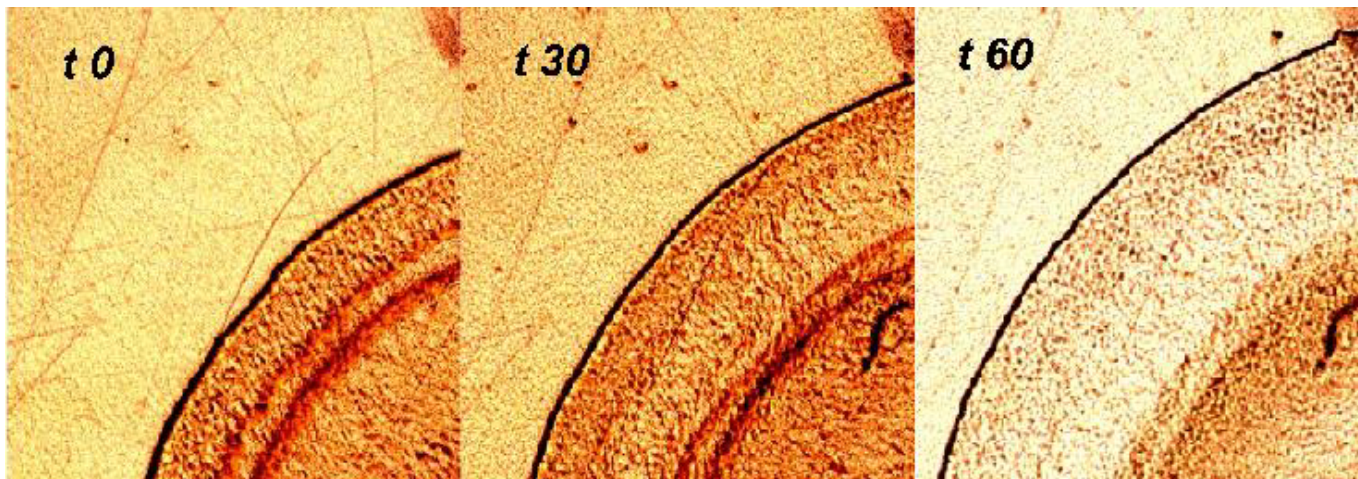


Figure 2: Active swarming phase on agar. The figure shows three snapshots 30 min apart during a migration phase on agar.

Proteus mirabilis swarm phenomenon has fascinated micro-biologists and other scientists for over a century, since Hauser [20] first described it. This fascination certainly comes from the fact that bacteria are often considered as very primitive organisms and from the astonishing fact that such primitive living forms are able to generate such nice regular structures. This phenomenon certainly played an important role in morphogenesis and fractal theories (see Thom [51], Mandelbrot [30], Falconer [14] and references in them) that highlighted in a very resounding way that very simple principles may generate very complex shapes. On the other hand, as explained by Kaufmann [22], phenomena of the *Proteus mirabilis* swarm kind seem to belong to an intermediary step between unicellular organisms and multicellular organisms. As a matter of fact, key elements to the understanding of evolution of life can certainly be found within the understanding of those phenomena.

Collective behaviour of bacteria colonies has been widely observed, described and studied. For instance, Hoeniger [21] delineated the *Proteus mirabilis* swarm phenomenon and Budrene & Berg [10] pointed out the ability that bacteria colonies have to draw complex patterns. Shapiro [42, 43, 44] and more recently Rauprich *et al.* [38] and Matsuyama *et al.* [33] made a wide observation campaign to precisely analyze the phenomenon.

This research effort pointed out that the swarm phenomenon has to be seen as an emergent property leading to the consideration of bacteria as multicellular organisms (see Shapiro & Dworkin [49], Shapiro [45, 48] and Dworkin [12]).

Research has mainly tackled the problems of origin and of regulation of bacterial collective behaviour with a genetic or a bio-chemical slant (see Shapiro [40, 41, 46, 47], Belas [7], Manos & Belas [31], Schneider *et al.* [39] and Gué *et al.* [17]).

The goal of the present paper is to add a bio-physical slant concerning the swarm phenomenon. More precisely, we exhibit the main physical phenomena of the bacteria to achieve their colonization. What we have chosen to do is to make assumptions about the physical principles governing the bacteria behaviour and controlling the swarm and to translate those assumptions into a mathematical model involving partial differential equations. Then, this model is implemented in Matlab[®]7 language. Using the resulting program, we make several simulations with several values of parameters involved in the model. We finally observe that macroscopic colony behaviours may be recovered by the simulations leading to the conclusion that our assumptions are not entirely unreasonable. Beyond this conclusion, the scientific approach consisting in using modelling and simulation in order to test assumptions, is another important contribution of this paper. We plan to apply it, in

forthcoming works, in order to refine *Proteus mirabilis* swarm explanation.

Using modelling, mathematical analysis and simulation to describe or understand biological systems is not unusual nowadays. For an introduction to these topics, we refer to Murray [37]. Those kinds of mathematical methods were applied in the context of collective behaviour of bacteria. For a description of this, we refer to Matsushita [32] and Ben-Jacob & Cohen [8].

Esipov & Shapiro [13] set out a kinetic model describing the swarm of *Proteus mirabilis* at the colony scale recovering the main behaviours of a real colony: time alternation of swarming phases and consolidation phases, time alternation of colony radius increases and stops and terraces. The key ingredient causing their model to produce good results is the introduction of an age structuring of the bacterial population as is suggested in Gurtin [18] and Gurtin & Mac Camy [19]. This introduction allows one to take into consideration the age of the swarmer cells when looking at their behaviour. This model was studied from mathematical and numerical analysis viewpoints in Esipov & Shapiro [13], Medvedev, Kapper & Koppel [35], Ayati [1, 2, 3, 4], Ayati & Dupont [5], Frénod [16], Ayati & Klapper [6] and Laurençot & Walker [26, 27]. In particular, Ayati [3] showed the importance of using age structured model to reproduce the cell size distribution pointed out by Matsuyama *et al.* [33].

The existing models describing colonization by bacteria generally contain an advection or diffusion term allowing one to define the direction in which the colony expands conformal to reality. This makes the model behave in a way which conforms to reality. But the factors in front of these advection and diffusion terms which control the beginning, velocity, and ending of the swarm are mainly set from phenomenological considerations.

As for the research of physical principles explaining bacterial collective behaviour we mention Mendelson, Salhi & Li [36].

Acknowledgements - We thank James Shapiro and Bruce Ayati who pointed out lacks in the first version of the paper and suggested ways to remedy them. We also thank Joanna Ropers for proofreading this paper.

2 Explanation of the principles governing the swarm

From a long *in situ* observation campaign of *Proteus mirabilis* colonies (see Gué *et al.* [17], Keirsse *et al.* [23], Lahaye *et al.* [24, 25]) and knowledge of physical phenomena arising within complex fluids, we are convinced that the main physical explanations of *Proteus mirabilis* swarm come from the properties of the extra cellular matrix which is the complex fluid smothering the bacteria of the colony. More than ten years ago, Rauprich *et al.* [38] hypothesised the key role of relative osmotic activities at the agar colony interface. More recently, Berg [9] and Chen *et al.* [11] further supported hypothesis of Lahaye *et al.* [24, 25] claiming that the preservation of a critical water concentration allowing swarming of bacteria colonies was due to an osmotic agent.

In short, two properties seem to play an important role: the thickness of the colony and the water concentration within the extra cellular matrix.

The colony thickness plays a role in controlling the growth rate of cells in their vegetative form: once a given thickness is reached, the cell division ends, stopping vegetative population growth.

The extra cellular matrix is compounded with water, polysaccharides and lipids. When the water concentration of this matrix is low, polysaccharides and lipids auto-organize which results in semi-crystallinity and visco-elastic properties. When it is high, polysaccharides and lipid auto-organization is lost, due to efficient solvent competition with solute-solute interactions, decreasing thereby the visco-elastic properties of the extra cellular matrix.

It has been well established that the translocation ability of the colony is a consequence of the rotation and oscillation the hundreds of flagella of a large number of swarmer cells. On the other hand, observations have put into light that consolidation phases begin despite numbers of swarmer cells are present and moving but without any effect on colony displacement.

Hence, we may infer that water concentration rules the swarm phenomenon in the following way. When it is low, swarmer cells interacting with visco-elastic properties of the extra cellular matrix produce colony expansion. When the matrix water concentration is high, the visco-elastic properties are lost. Then swarmer cell agitation, when it occurs, does not produce a swarm.

The differentiation process may be assumed to be a kind of dysfunction in the cell division process: for a small proportion of vegetative bacteria, the cell division is not brought to completion. It is also consistent to suppose that a cell having undergone this differentiation goes on elongating, as long as water concentration is low, until it reaches a maximum length depending on water concentration. Once this maximum length is reached, the cell oscillation and rotation begin. At this stage, the swarmer cells become almost metabolically dormant (see for instance Stickler [50], Mc Coy *et al.* [34] and Falkinham and Hoffman [15]) and then do not consume extra fuel from the extra cellular matrix during their migration. Then we may suppose that their life duration, in this stage, is finite and linked to their length. After their life duration, the metabolism-frozen swarmer cells de-differentiate to produce new vegetative cells.

In a given place of the colony, the evolution of water concentration of the extra cellular matrix is influenced by the density of bacteria, which need water to achieve metabolism, and by the displacement of swarmer cells which bring with them a part of their surrounding medium. The third factor influencing matrix water concentration is the water concentration in the agar medium with which it exchanges water and the corresponding transfer properties at the agar - colony interface.

3 Translation of the principles into a model

In this section, we translate the principles explained in the previous section into a model, in the simplest manner possible, and even in an oversimplified manner.

The model set out in Esipov & Shapiro [13] coupled two equations. The first of them was an ordinary differential equation describing the evolution of the vegetative cell biomass density. The swarmer cells were modelled by an age-structured density which was the solution to a partial differential equation describing aging, but also de-differentiation and swarming, both being age dependent processes.

The model we have set out in the present paper, involves three equations. The first concerns vegetative cells. To be able to take into account that the differentiated cells undergo an elongation phase, followed by a swarming phase with no metabolism, we consider an equation modelling the evolution of the elongating cells and another one modelling the evolution of swarmer cells having stopped their metabolism, both of them involving age-structured functions.

We begin by considering the evolution of the vegetative cells. For this, we introduce the function $Q(t, x)$ which is the vegetative cell biomass density at time $t \in [0, T)$ and in a given position $x \in \mathbb{R}^2$. It is supposed to be the solution to the following ordinary differential equation:

$$\frac{\partial Q}{\partial t} = \frac{1-\xi}{\tau} Q \chi\left(\frac{\bar{\mathcal{E}} - \mathcal{E}}{\bar{\mathcal{E}}}\right) \chi\left(\frac{Q - \bar{Q}}{\bar{Q}}\right) + \int_0^{+\infty} \rho(t, a, \kappa a, x) e^{a/\tau} da. \quad (3.1)$$

The time evolution of Q is the result of cell division, described by the first term on the right-hand side of the equation (3.1), and of the de-differentiation products quantified by the second term. In the first term, τ stands for the growth rate of the cell division process, ξ , $0 \leq \xi \leq 1$, is the proportion of cells undergoing differentiation, and then $1 - \xi$ is the proportion of cells bringing their division to completion. The function χ has the following definition $\chi(E) = 0$ if $E < 0$ and $= 1$ otherwise. Then the factor $\chi((\bar{\mathcal{E}} - \mathcal{E})/\bar{\mathcal{E}})$, where $\mathcal{E} = \mathcal{E}(t, x)$ is swarm colony thickness at t in x , takes into account the above evoked control of colony thickness on the cell division process in the following way: when $\mathcal{E} \geq \bar{\mathcal{E}}$, the term is set to 0. The factor $\chi((Q - \bar{Q})/\bar{Q})$ precludes the growth of Q by cell division when Q is too low, *i.e.* when $Q < \bar{Q}$.

In the second term, $\rho(t, a, b, x)$, at time $t \in [0, T)$, stands for the density of swarmer cells in position $x \in \mathbb{R}^2$, having been freezing their metabolism at an age $a \in [0, +\infty)$, for a period of time b . Since the life duration of the the swarmer cells in this state is supposed to be linked to their length and since the length of a given swarmer cell is linked to the duration during which it elongated, we set that the life duration of a swarmer cell having stopped metabolism at an age a is κa . The growth rate of the biomass of the elongating cells is the same as the one of the vegetative cells. Hence the biomass density in position x of swarmer cells having been stopping their metabolism at an age a , for a period of time b is $\rho(t, a, b, x) e^{a/\tau}$ and the integral in the second term on the right-hand side of (3.1) is nothing but the biomass density of cells that de-differentiate at time t .

The biomass density of vegetative cells at time $t = 0$ is given by the following initial data:

$$Q(0, x) = Q_0(x). \quad (3.2)$$

The description of the evolution of elongating cell population involves the following age-structured function $\zeta(t, a, x)$, which stands, at time $t \in [0, T)$, for the density of elongating cells of age $a \in [0, +\infty)$ in $x \in \mathbb{R}^2$. The evolution of this density is due to aging and to the transformation of elongating cells into swarmer cells. We assume that this transformation in a given position x takes place according to a transformation rate $\mu(a, H)$ depending on age a of the considered bacteria and on water concentration $H = H(t, x)$ of the matrix. The dependence of μ with respect to H takes into account that the lower H is, the larger the existence duration expectancy of elongating cells is.

The equation modelling the evolution of ζ is:

$$\frac{\partial \zeta}{\partial t} + \frac{\partial \zeta}{\partial a} = -\mu(a, H)\zeta. \quad (3.3)$$

Since the proportion ξ of vegetative cells that differentiate generates elongating cells with age 0, equation (3.1) and (3.3) are linked by the following transfer condition,

$$\zeta(t, 0, x) = \frac{\xi}{\tau} Q(t, x) \chi\left(\frac{\bar{\mathcal{E}} - \mathcal{E}}{\bar{\mathcal{E}}}\right) \chi\left(\frac{Q - \bar{Q}}{\bar{Q}}\right). \quad (3.4)$$

The elongating cell density at the initial time is given by:

$$\zeta(0, a, x) = \zeta_0(a, x), \quad (3.5)$$

Now we turn to the modelling of the evolution of the swarmer cells which have stopped their metabolism.

We consider that the velocity of swarmer cells is the consequence of the interaction of their agitation with the visco-elastic properties of the matrix when water concentration is low. Then we introduce a function $c(H)$ which is non-zero for the small value of H and with value 0 for the large value of H . Then, as the global motion of swarmer cells, when it exists, is the consequence of cell agitation it is reasonable to consider that their velocity is in proportion with the colony thickness gradient $\nabla \mathcal{E}$, the proportion coefficient being $c(H)$. In other words, we consider that the swarmer cell velocity in a given position x is $c(H(t, x))\nabla \mathcal{E}(t, x)$.

The definition of $\rho(t, a, b, x)$ defined for $t \in [0, T)$, $a \in [0, +\infty)$, $b \in [0, \kappa a)$ and $x \in \mathbb{R}^2$ was already given. In view of this definition, if S is a regular set of \mathbb{R}^2 and $b_1 < b_2 \leq \kappa a$ are two numbers,

$$\int_{S \times [b_1, b_2]} \rho(t, a, b, x) db dx, \quad (3.6)$$

is, at time t , the density of bacteria having stopped their metabolism at an age a , for a time larger than b_1 and smaller than b_2 and situated in S . The time evolution of this quantity is linked to the

aging fluxes in b_1 and b_2 and to the swarming flux on the boundary ∂S of S which has the following expression

$$\int_{\partial S \times [b_1, b_2]} (c(H) \nabla \mathcal{E} \rho) \cdot n \, dbdl, \quad (3.7)$$

where n stands for vector with norm 1, orthogonal to S and pointing outwards and where dl is the Lebesgue measure on ∂S . Hence we deduce the following equation:

$$\frac{d\left(\int_{S \times [b_1, b_2]} \rho \, dbdx\right)}{dt} = \int_S \rho(t, a, b_1, x) \, dx - \int_S \rho(t, a, b_2, x) \, dx - \int_{\partial S \times [b_1, b_2]} (c(H) \nabla \mathcal{E} \rho) \cdot n \, dbdl. \quad (3.8)$$

Using the divergence operator $\nabla \cdot$ to transform flux integral into integral over S and noticing that $\nabla \cdot (c(H) \nabla \mathcal{E} \rho) = c(H) \nabla \mathcal{E} \cdot \nabla \rho + \rho \nabla \cdot (c(H) \nabla \mathcal{E})$, we finally obtain the partial differential equation ρ satisfies:

$$\frac{\partial \rho}{\partial t} + \frac{\partial \rho}{\partial b} = -c(H) \nabla \mathcal{E} \cdot \nabla \rho - \rho \nabla \cdot (c(H) \nabla \mathcal{E}). \quad (3.9)$$

Since the elongating cells that stop metabolism at an age a become swarmer cells, we have the following transfer condition

$$\rho(t, a, 0, x) = \mu(a, H) \zeta, \quad (3.10)$$

and the following initial condition

$$\rho(t, 0, b, x) = \rho_0(t, b, x), \quad (3.11)$$

to provide (3.9) with.

The thickness \mathcal{E} of the colony in a given position is in direct proportion to the biomass density value at this point. In other words we set

$$\mathcal{E} = Q + \mathcal{M} + \mathcal{N}, \quad (3.12)$$

where

$$\mathcal{M}(t, x) = \int_0^{+\infty} \zeta(t, a, x) e^{a/\tau} \, da, \quad (3.13)$$

is the biomass density of elongating cells. Notice that $Q + \mathcal{M}$ is the biomass density of metabolic cells; and \mathcal{N} , defined as

$$\mathcal{N}(t, x) = \int_0^{+\infty} \int_0^{\kappa a} \rho(t, a, b, x) e^{a/\tau} \, dadb, \quad (3.14)$$

is the density of metabolically dormant cells.

We now turn to the description of water concentration evolution. We first consider the water concentration of agar gel near the contact surface. Let $G(t, x)$, defined for $t \in [0, T)$, $x \in \mathbb{R}^2$, be the value of this water concentration at time t and in position x . We consider that it evolves due to water transfers from and to the extra cellular matrix and that those transfers are proportional to the water concentration difference between the two media and to a colony thickness function. We name γ_t the proportion factor. There are also water exchanges between the agar layers close to the

contact surface and the deeper layers. We model those exchanges by a simple ability to relax to the concentration value being worth 1 with a velocity γ_d . In other words, we consider that G evolves according to the following equation:

$$\frac{\partial G}{\partial t} = -\gamma_t \mathcal{T}(\mathcal{E})(G - H) + \gamma_d(1 - G), \quad (3.15)$$

where $\mathcal{T}(\mathcal{E}) = \mathcal{E}$ if $\mathcal{E} \leq 1$ and $\mathcal{T}(\mathcal{E}) = 1$ otherwise. Equation (3.15) is equipped with the following initial data

$$G(0, x) = G_0(x), \quad (3.16)$$

giving water concentration of agar at initial time.

Since it is easier to model water quantity transfer as water concentration transfer, we introduce $h(t, x)$, defined for $t \in [0, T)$ and $x \in \mathbb{R}^2$ which is the water density contained within the matrix in position x at time t . This density is clearly proportional to the thickness of the colony times the water concentration, with a proportion factor η that is linked to the part of the swarm colony the matrix constitutes, *i.e.* $h = \eta \mathcal{E} H$.

If S is a regular subset of \mathbb{R}^2 with boundary ∂S equipped with the vector field n with norm 1 orthogonal to S and pointing outwards and with the Lebesgue measure dl , the quantity

$$\int_S h dx, \quad (3.17)$$

is the water quantity contained in the swarm colony over S . This quantity evolves according to

$$\begin{aligned} \frac{d\left(\int_S h dx\right)}{dt} = & - \int_S \left(\alpha - \left(1 - \chi\left(\frac{\bar{\mathcal{E}} - \mathcal{E}}{\bar{\mathcal{E}}}\right) \chi\left(\frac{Q - \bar{Q}}{\bar{Q}}\right)\right) \alpha' \right) Q dx - \int_S \alpha \mathcal{M} dx \\ & + \int_S \gamma_t \mathcal{T}(\mathcal{E})(G - H) dx - \int_{\partial S} (c(H) \nabla \mathcal{E} \eta \mathcal{N} H) \cdot n dl. \end{aligned} \quad (3.18)$$

The second term of the right-hand side of this equation quantifies the amount of water the elongating cells use for metabolism. This quantity is proportional, with a factor α , to the biomass density of elongating cells. The first term quantifies the amount of water used for metabolism by vegetative cells. This quantity is proportional to the biomass density of vegetative cells. The proportion factor is α when vegetative cells undergo cell division and is $\alpha - \alpha'$ when they do not undergo cell division, *i.e.* when $\chi((\bar{\mathcal{E}} - \mathcal{E})/\bar{\mathcal{E}})\chi((Q - \bar{Q})/\bar{Q}) = 0$. Since the swarmer cells are metabolically dormant, we consider they do not intervene in water consumption. The third term models the water exchanges with agar. The last term gives the flux of water carried by the swarmer cells. In it, $c(H) \nabla \mathcal{E}$ is the velocity of the swarmer cells and then of the medium they carry with them; $\eta \mathcal{N} H$ is the water quantity carried by the swarmer cells, it is proportional to the swarmer biomass and to the water concentration in the matrix.

Using the divergence operator, we deduce from (3.18) that h is solution to

$$\begin{aligned} \frac{\partial h}{\partial t} = & - \left(\alpha - \left(1 - \chi\left(\frac{\bar{\mathcal{E}} - \mathcal{E}}{\bar{\mathcal{E}}}\right) \chi\left(\frac{Q - \bar{Q}}{\bar{Q}}\right)\right) \alpha' \right) Q - \alpha \mathcal{M} \\ & + \gamma_t \mathcal{T}(\mathcal{E})(G - H) - \eta c(H) \nabla \mathcal{E} \cdot \nabla(\mathcal{N} H) - \eta \mathcal{N} H \nabla \cdot (c(H) \nabla \mathcal{E}), \end{aligned} \quad (3.19)$$

endowed with the following initial data

$$h(0, x) = h_0(x), \quad (3.20)$$

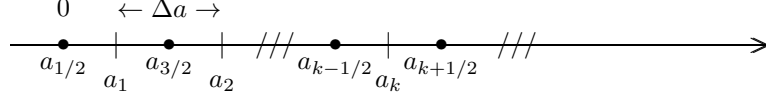


Figure 3: Elongating cell age axis discretization

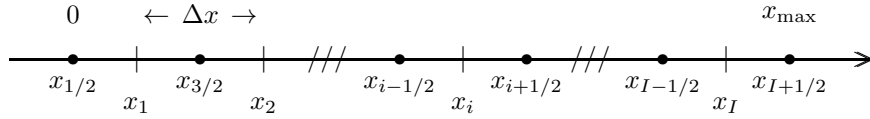


Figure 4: Position axis discretization

describing the water density at time $t = 0$.

From the link between H and h , we deduce

$$\frac{\partial h}{\partial t} = \eta \left(H \frac{\partial \mathcal{E}}{\partial t} + \mathcal{E} \frac{\partial H}{\partial t} \right), \quad (3.21)$$

and then, from equation (3.19), an equation for H

$$\begin{aligned} \frac{\partial H}{\partial t} = & -\frac{H}{\mathcal{E}} \frac{\partial \mathcal{E}}{\partial t} - \frac{1}{\eta} \left(\alpha - \left(1 - \chi \left(\frac{\bar{\mathcal{E}} - \mathcal{E}}{\bar{\mathcal{E}}} \right) \chi \left(\frac{Q - \bar{Q}}{\bar{Q}} \right) \right) \alpha' \right) \frac{Q}{\mathcal{E}} \\ & - \frac{\alpha \mathcal{M}}{\eta \mathcal{E}} + \frac{\gamma_t \mathcal{T}(\mathcal{E})}{\eta \mathcal{E}} (G - H) - \frac{c(H)}{\mathcal{E}} \nabla \mathcal{E} \cdot \nabla (\mathcal{N}H) - \frac{\mathcal{N}}{\mathcal{E}} H \nabla \cdot (c(H) \nabla \mathcal{E}), \end{aligned} \quad (3.22)$$

$$H(0, x) = H_0(x) = \frac{h_0(x)}{\eta \mathcal{E}}. \quad (3.23)$$

4 Implementation

From the model just set out, we write a Biomass Preserving Finite Volume-like numerical scheme (see LeVeque [28, 29]) and then we implement it.

In this section, to simplify matters, we consider the swarm of a *Proteus mirabilis* population whose distribution remains independent of the second position variable and an agar medium which is also independent of the second position variable. This means that the position space is considered nothing but a segment, say $[0, x_{\max}]$, of \mathbb{R} . We introduce a time step Δt , and age steps Δa and Δb with the following link $\Delta b = \Delta a = \Delta t$. We also define a position step Δx such that, $I \Delta x = x_{\max}$, for an integer I . We then define, for $n \in \mathbb{N}$, $t_n = n \Delta t$, for $k \in \mathbb{N}^*$, $a_k = (k - 1/2) \Delta a$ (see Figure 3), for $p \in \mathbb{N}^*$, $b_p = (p - 1/2) \Delta b$, and, for $i \in \{1, \dots, I\}$, $x_i = (i - 1/2) \Delta x$ (see Figure 4).

For every t_n , the function $Q(t_n, \cdot)$ is approximated by a function with a constant value, defined as Q_i^n , on every interval $(x_{i-1/2}, x_{i+1/2})$, where $x_{i-1/2} = x_i - \Delta x/2 = (i - 1) \Delta x$ and $x_{i+1/2} = x_i + \Delta x/2 = i \Delta x$ for $i \in \{1, \dots, I\}$. Consistently, the approximation of initial data (3.2) is:

$$Q_i^0 = \frac{1}{\Delta x} \int_{x_{i-1/2}}^{x_{i+1/2}} Q_0(x) dx. \quad (4.1)$$

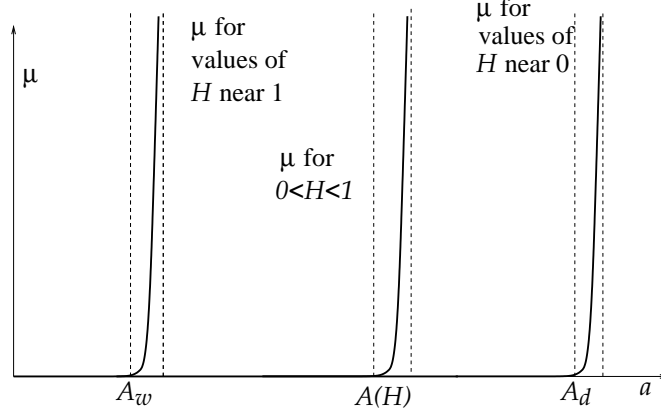


Figure 5: Shapes of μ for matrix with high, medium or low water concentration.

Equation (3.1) is approximated by

$$Q_i^{n+1} = Q_i^n + \Delta t \left(\frac{1-\xi}{\tau} Q_i^n \chi\left(\frac{\bar{\mathcal{E}} - \mathcal{E}_i^n}{\bar{\mathcal{E}}}\right) \chi\left(\frac{Q_i^n - \bar{Q}}{\bar{Q}}\right) + \mathcal{D}_i^n \right), \quad (4.2)$$

where \mathcal{E}_i^n and \mathcal{D}_i^n are approximations of the mean values of $\mathcal{E}(t_n, \cdot)$ and of $\int_0^{+\infty} \rho(t_n, a, \kappa a, \cdot) e^{a/\tau} da$ over $(x_{i-1/2}, x_{i+1/2})$, supposed to be available and defined in the sequel.

The function $\zeta(t_n, \cdot, \cdot)$ is then approached by a function $\tilde{\zeta}(t_n, \cdot, \cdot)$, which is constant, with worth $\zeta_{k,i}^n$, on any rectangle $\mathcal{R}_{k,i} = (a_{k-1/2}, a_{k+1/2}) \times (x_{i-1/2}, x_{i+1/2})$, where $a_{k-1/2} = a_k - \Delta a/2 = (k-1)\Delta a$ and $a_{k+1/2} = a_k + \Delta a/2 = k\Delta a$, such that

$$\int_{\mathcal{R}_{k,i}} \tilde{\zeta}(t_n, a, x) e^{a/\tau} dadx = \Delta x (e^{k\Delta a/\tau} - e^{(k-1)\Delta a/\tau}) \tau \zeta_{k,i}^n$$

is supposed to be close to $\int_{\mathcal{R}_{k,i}} \zeta(t_n, a, x) e^{a/\tau} dadx$, (4.3)

for $k \in \mathbb{N}^*$ and $i \in \{1, \dots, I\}$. Then, the approximation of initial data (3.5) reads

$$\zeta_{k,i}^0 = \frac{1}{\Delta x (e^{k\Delta a/\tau} - e^{(k-1)\Delta a/\tau}) \tau} \int_{\mathcal{R}_{k,i}} \zeta_0(a, x) e^{a/\tau} dadx. \quad (4.4)$$

At each time step t_n , $\zeta_{0,i}^n$ for $i \in \{1, \dots, I\}$ are used for the biomass transfer from vegetative cells. Hence we translate condition (3.4) into:

$$\zeta_{0,i}^n = \frac{\Delta t}{(e^{\Delta a/\tau} - 1) \tau} \frac{\xi}{\tau} Q_i^n \chi\left(\frac{\bar{\mathcal{E}} - \mathcal{E}_i^n}{\bar{\mathcal{E}}}\right) \chi\left(\frac{Q_i^n - \bar{Q}}{\bar{Q}}\right). \quad (4.5)$$

We introduce a non increasing function $A(H)$, ranging in the interval $[A_w, A_d]$ with $A(0) = A_d$ and $A(1) = A_w$, and before approximating (3.3) we assume that for any value of H , function $\mu(\cdot, H)$ is 0 when $a \leq A(H)$ and increases very quickly after this value, as illustrated in Figure 5. In other words, we assume that at a given value H of the water concentration, the elongating cells remain in there state until an age $A(H)$ and that they become swarmer cells very soon after this age. With this assumption and since $\Delta a = \Delta t$, equation (3.3) may be approximated by:

$$\zeta_{k,i}^{n+1} = \zeta_{k-1,i}^n, \text{ for every } i \in \{1, \dots, I\} \text{ and every } k \in \mathbb{N}^* \text{ such that } (k-1/2)\Delta a \leq A(H_i^n), \quad (4.6)$$

$$\zeta_{k,i}^{n+1} = 0, \text{ for every } i \in \{1, \dots, I\} \text{ and every } k \in \mathbb{N}^* \text{ such that } (k-1/2)\Delta a > A(H_i^n), \quad (4.7)$$

where H_i^n is an approximation of H near x_i at time t_n to be defined hereafter.

We now turn to the swarmer cells. We approximate their density $\rho(t_n, \cdot, \cdot)$ by a function $\tilde{\rho}$ which is constant on any parallelepiped $\mathcal{P}_{k,p,i} = (a_{k-1/2}, a_{k+1/2}) \times (b_{p-1/2}, a_{p+1/2}) \times (x_{i-1/2}, x_{i+1/2})$. The value $\rho_{k,p,i}^n$ is defined as being such that $\Delta b \rho_{k,p,i}^n$ is the value of $\tilde{\rho}$ on this parallelepiped. Consistent with this definition, initial data (3.11) is approximated by

$$\rho_{k,p,i}^0 = \frac{1}{\Delta x (e^{k\Delta a/\tau} - e^{(k-1)\Delta a/\tau})_\tau} \int_{\mathcal{P}_{k,p,i}} \rho_0(a, b, x) e^{a/\tau} da db dx. \quad (4.8)$$

Transfer condition (3.10) is approached by:

$$\rho_{k,0,i}^{n+1} = \sum_{(k-1/2)\Delta a > A(H_i^n)} \zeta_{k,i}^n, \quad (4.9)$$

for every $i \in \{1, \dots, I\}$, this last relation balancing (4.7).

To be able to obtain a biomass preserving scheme, we chose to discretize the form (3.8) of the equation giving the evolution of ρ . We make a splitting that consists in sequentially processing aging, the action of which is quantified by the two first terms on the right-hand side of equation (3.8), and, translocation modelled by the last term.

The first step of the splitting that takes into account aging, consists simply in introducing a sequence $(\rho_{k,p,i}^{n+1/2})$ for $k \in \mathbb{N}^*$, $p \in \mathbb{N}^*$ and $i \in \{1, \dots, I\}$ defined by

$$\rho_{k,p,i}^{n+1/2} = \rho_{k,p-1,i}^n. \quad (4.10)$$

For the second step of the splitting we need an approximation of the flux velocity $c(H)\nabla\mathcal{E}$ at all points $x_{i-1/2} = (i-1)\Delta x$ which are defined for $i \in \{1, \dots, I+1\}$, and which are the interfaces between the discretization interval $(x_{i-1/2}, x_{i+1/2})$ of the position space. Calling $V_{i-1/2}^n$ the value of this approximation, we set $i \in \{2, \dots, I\}$

$$V_{i-1/2}^n = c \left(\frac{2}{\frac{1}{H_{i-1}^n} + \frac{1}{H_i^n}} \right) \frac{1}{\Delta x} (\mathcal{E}_i^n - \mathcal{E}_{i-1}^n), \quad (4.11)$$

that allows one to minimize retrograde polluting propagation of the flux in regions where its velocity is zero. We set $V_{1/2}^n = 0$ and $V_{I+1/2}^n = V_{I-1/2}^n$ which makes the swarmer cells go out of the domain boundary once they have reached it.

From those flux velocities, we define the swarmer fluxes $F_{k,p,i-1/2}^n$ in all interfaces $x_{i-1/2}$. In an interface where the velocity is non negative, the value of the swarmer density just before the interface is taken into account. In an interface where the velocity is non positive, the value of the swarmer density just after the interface is taken into account. In other words we set:

$$\begin{aligned} F_{k,p,i-1/2}^n &= V_{i-1/2}^n \rho_{k,p,i}^{n+1/2} & \text{if } V_{i-1/2}^n \leq 0, \\ F_{k,p,i-1/2}^n &= V_{i-1/2}^n \rho_{k,p,i-1}^{n+1/2} & \text{if } V_{i-1/2}^n > 0. \end{aligned} \quad (4.12)$$

Once the fluxes are computed, not forgetting that ρ is defined for values of b smaller than κa and that swarmer cells at an age $b = \kappa a$ de-differentiate to produce vegetative cells, the values of the swarmer density approximation for the next time step is given, for every $i \in \{1, \dots, I\}$, by

$$\rho_{k,p,i}^{n+1} = \rho_{k,p,i}^{n+1/2} + \frac{\Delta t}{\Delta x} (F_{k,p,i-1/2}^n - F_{k,p,i+1/2}^n), \quad (4.13)$$

for every $p \in \mathbb{N}^*$ and $k \in \mathbb{N}^*$ such that $(p-1/2)\Delta b \leq \kappa(k-1/2)\Delta a$,

$$\rho_{k,p,i}^{n+1} = 0, \text{ for every } p \in \mathbb{N}^* \text{ and } k \in \mathbb{N}^* \text{ such that } (p-1/2)\Delta b > \kappa(k-1/2)\Delta a, \quad (4.14)$$

and the approximation \mathcal{D}_i^{n+1} of $\int_0^{+\infty} \rho(t_{n+1}, a, \kappa a, \cdot) e^{a/\tau} da$ available for the next time step, by

$$\mathcal{D}_i^{n+1} = \sum_{(p-1/2)\Delta b > \kappa(k-1/2)\Delta a} \left(\rho_{k,p,i}^{n+1/2} + \frac{\Delta t}{\Delta x} (F_{k,p,i-1/2}^n - F_{k,p,i+1/2}^n) \right) (e^{k\Delta a/\tau} - e^{(k-1)\Delta a/\tau}) \tau. \quad (4.15)$$

In every formula above the approximation (\mathcal{E}_i^n) of the thickness \mathcal{E} is given, for $i \in \{1, \dots, I\}$, by

$$\mathcal{E}_i^n = Q_i^n + \mathcal{M}_i^n + \mathcal{N}_i^n, \quad (4.16)$$

$$\mathcal{M}_i^n = \sum_{k \in \mathbb{N}^*} (e^{k\Delta a/\tau} - e^{(k-1)\Delta a/\tau}) \tau \zeta_{k,i}^n, \quad (4.17)$$

$$\mathcal{N}_i^n = \sum_{(p-1/2)\Delta b \leq \kappa(k-1/2)\Delta a} (e^{k\Delta a/\tau} - e^{(k-1)\Delta a/\tau}) \tau \rho_{k,p,i}^n, \quad (4.18)$$

in accordance with (3.12), (3.13) and (3.14).

Function $G(t_n, \cdot)$ is approximated by a function which is constant on each interval $(x_{i-1/2}, x_{i+1/2})$. Equation (3.15) and initial data (3.16) are approached by

$$G_i^{n+1} = G_i^n - \Delta t \gamma_t \mathcal{T}(\mathcal{E}_i^n)(G_i^n - H_i^n) + \Delta t \gamma_d (1 - G_i^n), \quad (4.19)$$

$$G_i^0 = \frac{1}{\Delta x} \int_{x_{i-1/2}}^{x_{i+1/2}} G_0(x) dx. \quad (4.20)$$

Finally, we approximate the evolution of the water quantity by

$$\begin{aligned} h_i^{n+1} = h_i^n - \Delta t \left(\alpha - \left(1 - \chi \left(\frac{\bar{\mathcal{E}} - \mathcal{E}_i^n}{\bar{\mathcal{E}}} \right) \chi \left(\frac{Q_i^n - \bar{Q}}{\bar{Q}} \right) \right) \alpha' \right) Q_i^n - \Delta t \alpha \mathcal{M}_i^n \\ + \Delta t \gamma_t \mathcal{T}(\mathcal{E}_i^n)(G_i^n - H_i^n) + \frac{\Delta t}{\Delta x} (\tilde{F}_{i-1/2}^n - \tilde{F}_{i+1/2}^n) \end{aligned} \quad (4.21)$$

where, $V_{i-1/2}^n$ being defined by (4.11),

$$\begin{aligned} \tilde{F}_{i-1/2}^n &= \eta V_{i-1/2}^n \mathcal{N}_i^n H_i^n \quad \text{if } V_{i-1/2}^n \leq 0, \\ \tilde{F}_{i-1/2}^n &= \eta V_{i-1/2}^n \mathcal{N}_{i-1}^n H_{i-1}^n \quad \text{if } V_{i-1/2}^n > 0, \end{aligned} \quad (4.22)$$

and where h_i^n is the value of the constant by interval approximation of $h(t_n, \cdot)$ on $(x_{i-1/2}, x_{i+1/2})$. We then get H_i^{n+1} by

$$H_i^{n+1} = \frac{h_i^{n+1}}{\eta \mathcal{E}_i^{n+1}}. \quad (4.23)$$

The scheme just built was implemented in Matlab[®]7 language.

5 Simulations

In this section we present several simulations for various values of the given parameters. Those simulations lead to the conclusion that characteristics of the *Proteus mirabilis* colony can be recovered by the model just built.

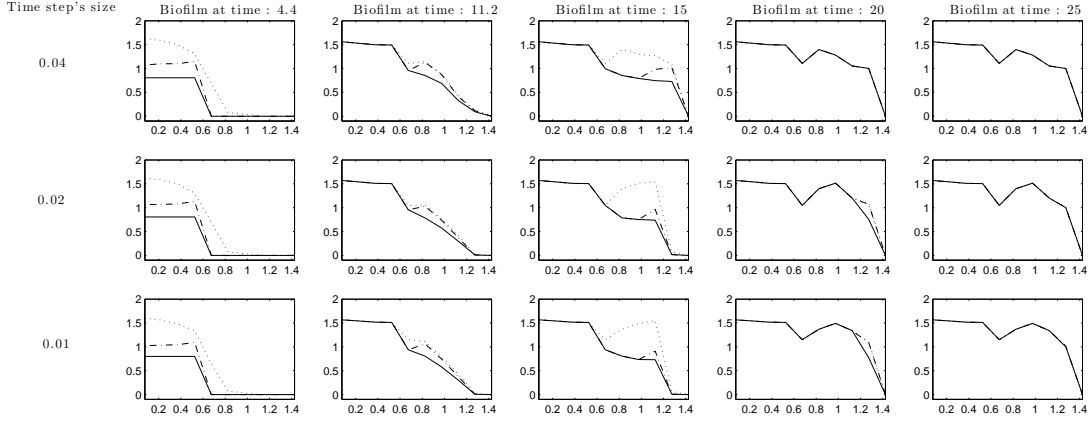


Figure 6: *Simulation 1 - Generation of two terraces with different time steps.*

5.1 Simulation 1

The goal of this first simulation is to show the ability of the model to generate terraces and to study the stability of terrace generation with respect to time step. We set the following values of the parameters

$$\begin{aligned} \xi = 0.1, \quad \tau = 1, \quad \bar{\mathcal{E}} = 1, \quad \bar{Q} = 0.2, \quad \gamma_t = 0.5, \quad \gamma_d = 0.9, \\ \eta = 0.5, \quad A_w = 1, \quad A_d = 3.5 \quad \kappa = 2, \quad \alpha = 0.3, \quad \alpha' = 0.28, \end{aligned} \quad (5.1)$$

we take as coefficient $c(H)$ involved in swarmer cell velocity

$$c(H) = 0.2 \text{ if } H < 0.5 \text{ and } 0 \text{ if } H \geq 0.5, \quad (5.2)$$

as position domain $[0, x_{\max}] = [0, 1.5]$, and as initial functions

$$Q_0(x) = 0.1 \text{ if } x \leq 0.6 \text{ and } 0 \text{ otherwise,} \quad (5.3)$$

$$\zeta_0(a, x) = 0 \text{ for all } a \in [0, +\infty) \text{ and } x \in [0, 1.5], \quad (5.4)$$

$$\rho_0(a, b, x) = 0 \text{ for all } a \in [0, +\infty), b \in [0, +\infty) \text{ and } x \in [0, 1.5]. \quad (5.5)$$

The initial water concentration in the extra cellular matrix is set to 0.7 and the initial water concentration in agar is set to 1. The position step is set to $\Delta x = 0.15$ leading to a value of $I = 11$ and simulations are done with values of Δt set to 0.04, 0.02 and 0.01, with $\Delta a = \Delta b = \Delta t$. The results associated with those values of Δt are given in figure 6 (line 1 gives the result for $\Delta t = 0.04$, line 2 gives the result for $\Delta t = 0.02$ and line 3 gives the result for $\Delta t = 0.01$). In each frame of this figure, the horizontal axis is the position axis and the vertical one gives the biomass densities. The solid line is the vegetative cell density Q , the dotted line represents the sum of the vegetative cell density and of the elongating cell biomass density $Q + \mathcal{M}$ if the latter is non zero. The dashed line is the sum of the vegetative cell density, of the elongating cell biomass density and of the swarmer cell biomass density $Q + \mathcal{M} + \mathcal{N}$, if the latter is non zero.

We see that for the three values of the time step, the dynamics of the colony and its final shape are similar. The more significant differences (see last column) are located near $x = 1.5$. Those differences are due to the influence of the boundary condition and certainly also to a numerical drift linked to the fact that this part of the colony is generated after a long term evolution.

Moreover, from a quantitative point of view, if $\mathcal{E}_i^n(\Delta t = 0.01)$ denotes the thickness of the colony at time t_n and in position x_i for the simulation made with $\Delta t = 0.01$, we have

$$\frac{\Delta x}{x_{\max}} \sqrt{\sum_{i=1}^I (\mathcal{E}_i^{25}(\Delta t = 0.02) - \mathcal{E}_i^{25}(\Delta t = 0.04))^2} = 0.0284, \quad (5.6)$$

$$\frac{\Delta x}{x_{\max}} \sqrt{\sum_{i=1}^I (\mathcal{E}_i^{25}(\Delta t = 0.01) - \mathcal{E}_i^{25}(\Delta t = 0.02))^2} = 0.0181, \quad (5.7)$$

suggesting that when values of time step has an order of magnitude of 0.01 or 0.02 we are not far from the stability of the swarm colony dynamics with respect to time step.

5.2 Simulation 2

The second simulation we present, consists in setting the following values of the parameters

$$\begin{aligned} \xi = 0.007, \quad \tau = 1, \quad \bar{\mathcal{E}} = 1, \quad \bar{Q} = 0.05, \quad \gamma_t = 0.03, \quad \gamma_d = 0.07, \\ \eta = 0.3, \quad A_w = 1, \quad A_d = 6.3 \quad \kappa = 2.5, \quad \alpha = 0.02, \quad \alpha' = 0.0194, \end{aligned} \quad (5.8)$$

in taking as coefficient $c(H)$ involved in swarmer cell velocity the function defined by (5.2), in taking as position domain $[0, x_{\max}] = [0, 4.5]$, and in taking as initial functions

$$Q_0(x) = 0.7 \text{ if } x \leq 0.6 \text{ and } 0 \text{ otherwise,} \quad (5.9)$$

$$\zeta_0(a, x) = 0 \text{ for all } a \in [0, +\infty) \text{ and } x \in [0, 4.5], \quad (5.10)$$

$$\rho_0(a, b, x) = 0 \text{ for all } a \in [0, +\infty), b \in [0, +\infty) \text{ and } x \in [0, 4.5]. \quad (5.11)$$

The initial water concentration in the extra cellular matrix is set to 0 and the initial water concentration in agar is set to 1.

Concerning the discretization parameters, $\Delta t = \Delta a = \Delta b = 0.05$, $\Delta x = 0.15$ leading to a value of $I = 30$. The simulation is provided over 3000 time steps or, in other words, over the time interval $[0, 150]$.

The beginning of the swarm phenomenon is summarized in Figure 8. This figure is divided into six pictures which are in turn divided into three frames. The top frame shows the biomass densities at the time given just above it. The horizontal axis is the position axis and the vertical one gives the biomass densities. The solid line is the vegetative cell density Q , the dotted line represents the sum of the vegetative cell density and of the elongating cell biomass density $Q + \mathcal{M}$ if the latter is non zero. The dashed line is the sum of the vegetative cell density, of the elongating cell biomass density and of the swarmer cell biomass density $Q + \mathcal{M} + \mathcal{N}$, if the latter is non zero. As a matter of fact, for instance, in the second picture the amount between the solid line and the dashed line has to be interpreted as the elongating cell biomass density; and, in the third picture the amount between the solid line and the dotted line has to be interpreted as the swarmer cell biomass density. The middle frame gives the water concentration H , ranging between 0 and 1, in the extra cellular matrix. The bottom frame shows the water concentration G in agar.

The first picture shows the situation at time 0.45. From the initial time on, the vegetative cell density has increased which has induced a water consumption proportional to the vegetative cell density with the proportion factor being α . As a consequence, at that time, the extra cellular matrix is very dry. Hence, the elongating cells which are created have a long existence duration expectancy. At the given time, the thickness just reaches 1. Hence the cell division stops and the only way for the colony thickness to grow is to increase the elongating cell biomass density. This is made possible by the elongation of each elongating cell, the mass of which then grows, and by the fact that elongating cells have a large life expectancy.

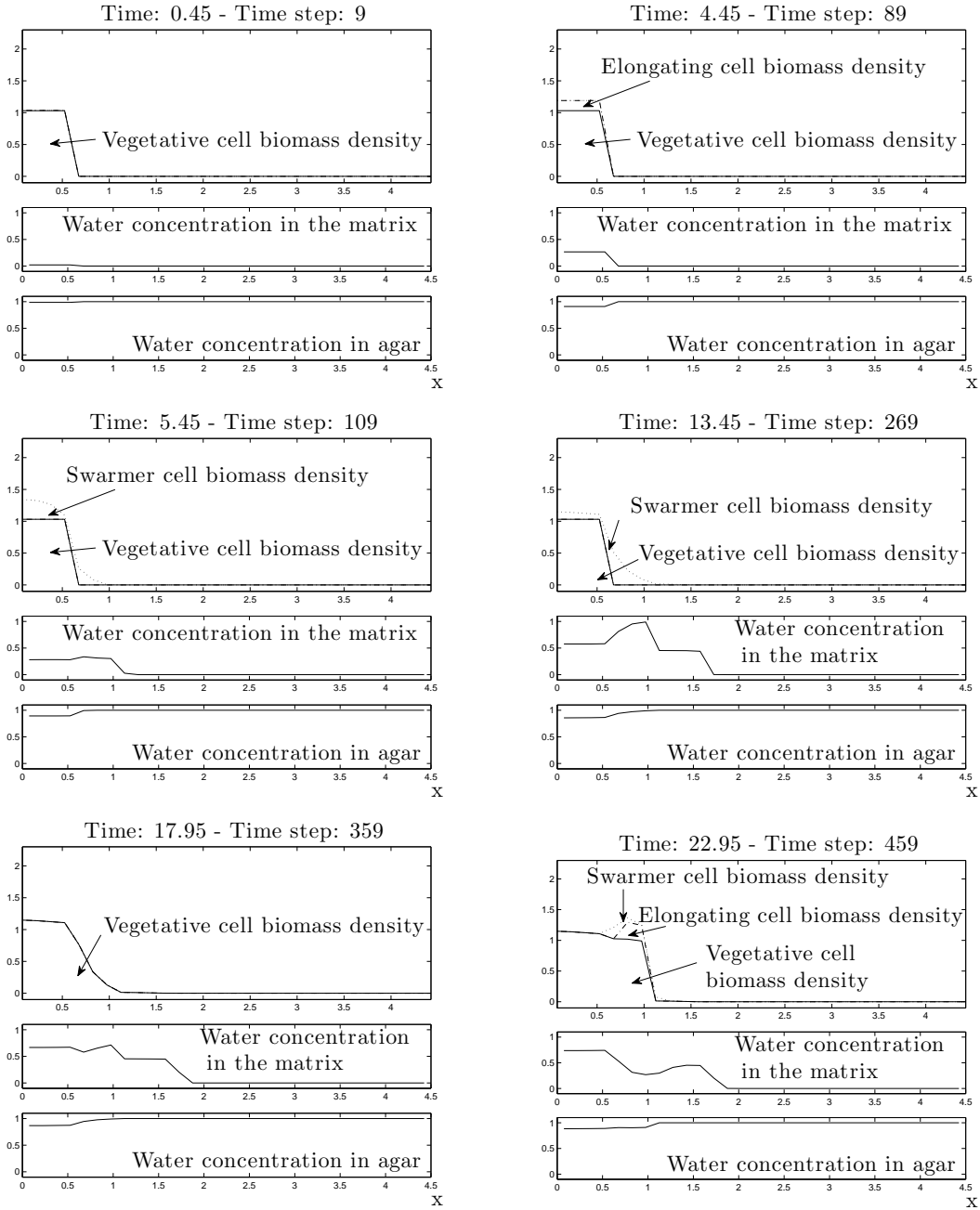


Figure 7: *Simulation 2 - Beginning of the swarm phenomenon: generation of the first terrace.*

The second picture shows the situation at time 4.45. Since time 0.45, the elongating cell biomass density, and the colony thickness have been increasing. The water concentration in agar has decreased little due to exchange with the extra cellular matrix. In the extra cellular matrix, the water consumed by vegetative cells is proportional to the vegetative cell density with the proportion factor being $\alpha - \alpha'$. The water consumed by elongating cells is proportional to the elongating cell biomass density with the proportion factor being α . As a result of the water consumption and exchanges, at this particular time, the extra cellular matrix is little hydrated. Soon after time 4.45, elongating cells become swarmer cells and, as the extra cellular matrix water concentration is low, the first swarm step begins.

The situation at time 5.45 (see third picture) is the following: the first swarm step is taking place and then swarmer cells move towards the positive x -axis. At the same time, the extra cellular matrix water concentration near $x = 0.8$, *i.e.* near the colony edge, is increasing faster than near the colony center. As a consequence, soon after time 5.45 the extra cellular matrix water concentration near the colony edge goes beyond the threshold $H = 0.5$ stopping swarmer cells, and then jamming the first swarm step.

Between time 5.45 and time 13.45 (see fourth picture), the swarm colony shape has not evolved a great deal. This period of time has to be interpreted as the first consolidation phase. The space distribution of the cell size, in accordance with Matsuyama *et al.* [33], shows a large proportion of long cells in the colony front and a smaller proportion in the colony interior. On the other hand, the extra cellular matrix water concentration has grown. In particular the threshold $H = 0.5$ has been overtaken in the colony center, which will prevent the swarm from going towards the colony center while the next swarm step begins.

At time 17.45 the first consolidation phase ends (see fifth picture). Since time 13.45, every swarmer cell has been de-differentiating to produce new vegetative cells, making the proportion of short cells to increase gradually, always in accordance with Matsuyama *et al.* [33]. As the total biomass density (or the thickness), near the colony edge, is low the cell division process may happen giving rise to an increase of vegetative cell density. At the same time, as the water consumption is important (proportional to the vegetative cell density with proportion factor α), the water concentration of the extra cellular matrix decreases fast.

At time 22.95 (see sixth picture), near $x = 1$, the extra cellular matrix water concentration is low. Hence the elongating cell existence duration expectancy is long. This leads to an increase in thickness, despite that the thickness is larger than 1. Elongating cells turn into swarmer cells which cannot go towards the colony center because of the high extra cellular matrix water concentration in this region. Hence they go towards positive x -axis, beginning the second swarm step.

Figure 8 depicts the generation of a terrace in the middle of the swarm phenomenon.

The situation in the first picture (time 60.65) is very similar to the one in the sixth picture of Figure 7: thickness is larger than 1, thickness increases due to elongating cells, elongating cells turn into swarmer cells, relative dryness of the extra cellular matrix near the colony edge and relative wetness of the extra cellular matrix while going towards the colony center which prevent swarming in that direction.

The second picture (time 63.45) shows the situation at the end of the swarm step, *i.e.* at the beginning of the consolidation phase. The characteristics of this moment are: wetness of the extra cellular matrix near the colony edge and in the colony center, relative dryness with increasing water concentration of the extra cellular matrix between the colony edge and the the colony center.

The colony shape has not evolved much between time 63.45 and time 73.45 (third picture) but the extra cellular matrix water concentration has increased. At time 73.45 the de-differentiation of swarmer cells is just beginning and producing vegetative cells, the population of which is growing by cell division. Here again, in accordance with Matsuyama *et al.* [33], a large proportion of long cells is present in the colony front and gradually this proportion decreases with time.

The water consumption is linked to the increase yield of a relatively dry extra cellular matrix near the colony edge, preparing the next swarm step beginning at time 75.45 (see forth picture).

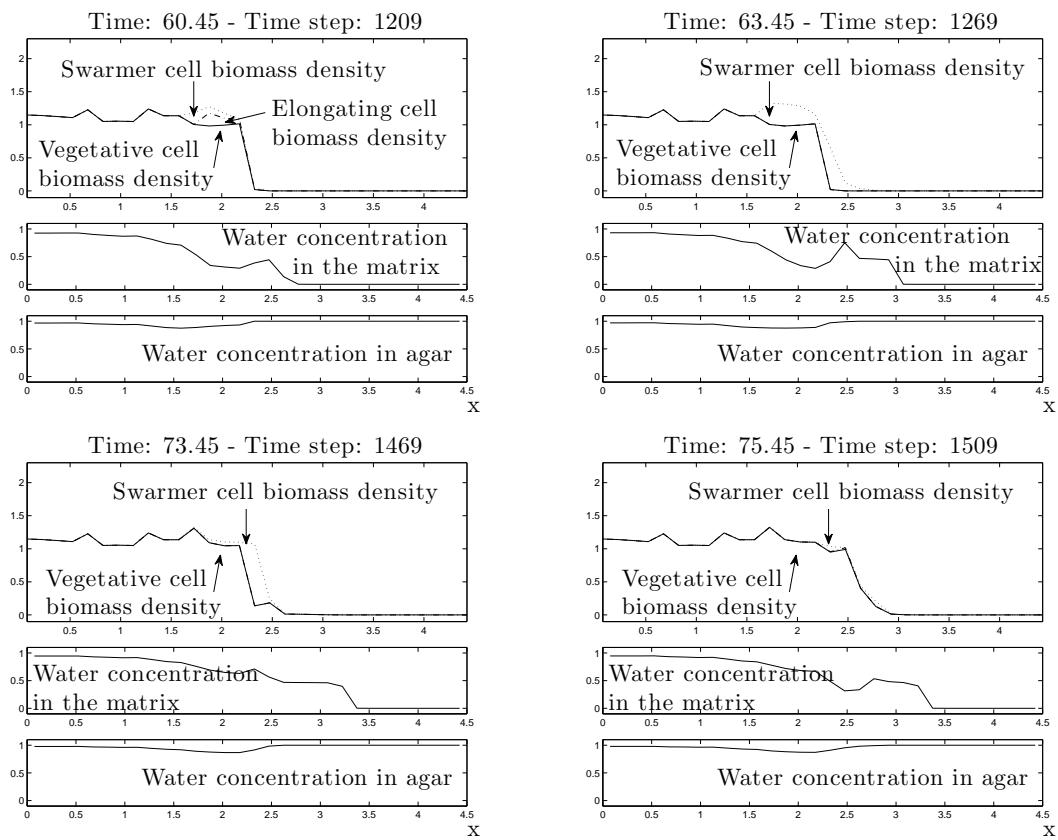


Figure 8: *Simulation 2 - Generation of a terrace in the middle of the swarm phenomenon.*

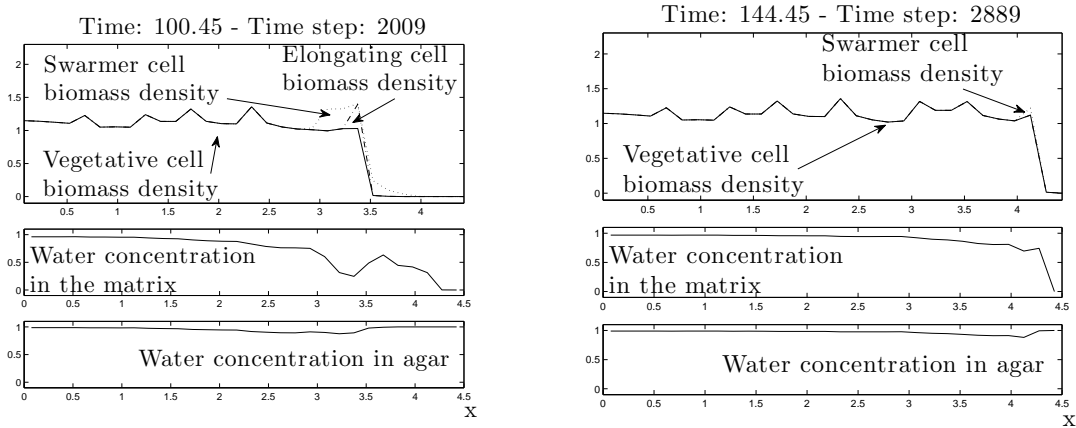


Figure 9: *Simulation 2 - End of the colonization.*

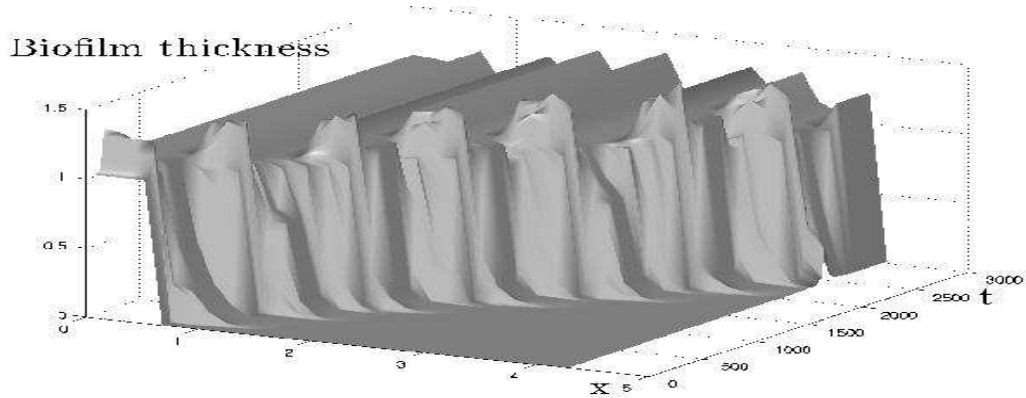


Figure 10: *Simulation 2 - Summarize of the swarm phenomenon.*

In the third and fourth pictures we can see that a remaining hump around $x = 1.7$ has been created during the time period covered by the pictures of Figure 8. This hump constitutes a terrace.

This colonization goes on until the whole position domain is conquered. Figure 9 shows the situation at time 100.45 and close to the end of the colonization process. The relative regularity of the terraces can be observed in these two pictures. We can also notice that the water concentration in agar and in the matrix slowly goes to 1.

Figure 10 summarizes the swarm phenomenon over the time period $[0, 150]$ *i.e.* from 0 to the 3000th time step. The horizontal axis going backward shows the time (in time step units) and the horizontal axis going to the right shows the position. The vertical axis represents the total biomass or thickness $Q + M + N$. This figure illustrates the relative regularity of the phenomenon, in time and position.

Moreover, it also allows one to visualize how the terraces are formed: a large hump is generated. Then it drains towards the colony edge but only partially, giving rise to a remaining hump which makes a terrace.

Finally, the first frame of Figure 11 shows the same object as in Figure 10 but restrained to time

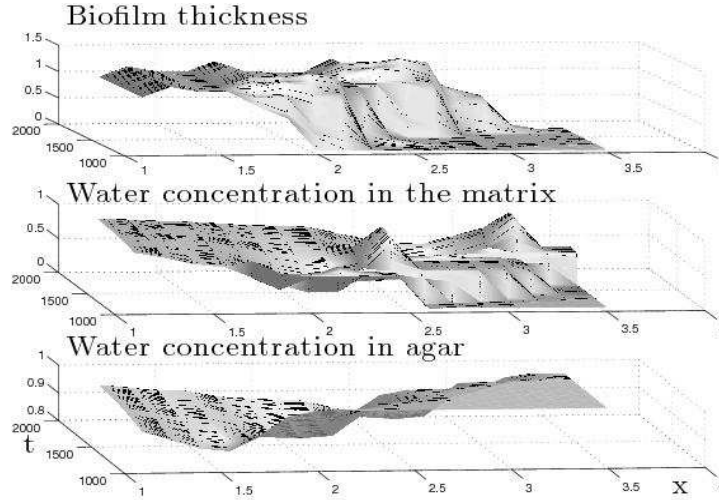


Figure 11: *Simulation 2 - Visualization of the relative positions of terraces, matrix water concentration maxima and agar water concentration minima.*

interval $[1000\Delta t, 2000\Delta t] = [50, 100]$. The second frame shows the water concentration in the extra cellular matrix and the third one shows the water concentration in agar.

This figure shows that, during the terrace formation, in front of the hump, the water concentration in the extra cellular matrix is high; and that, at the back of the hump, the water concentration in agar is low.

5.3 Simulation 3

The third simulation we present is carried out with the same position domain as before, with:

$$\xi = 0.008, \quad \tau = 1, \quad \bar{\mathcal{E}} = 1, \quad \bar{Q} = 0.05, \quad \gamma_t = 0.37, \quad \gamma_d = 0.13, \quad (5.12)$$

$$\eta = 0.3, \quad A_w = 1.2, \quad A_d = 5.5, \quad \kappa = 2.5, \quad \alpha = 0.42, \quad \alpha' = 0.41, \quad (5.13)$$

$$Q_0(x) = 0.2 \text{ if } x \leq 0.6 \text{ and } 0 \text{ otherwise,} \quad (5.13)$$

function ζ_0 given by (5.10), ρ_0 by (5.11) and c by (5.2). The initial water concentration in the extra cellular matrix is set to 0.8 and the initial water concentration in agar is set to 1.

The steps are $\Delta t = \Delta a = \Delta b = 0.05$, $\Delta x = 0.15$ leading to a value of $I = 30$. The simulation is provided over 4400 time steps or over the time interval $[0, 220]$.

Some parameters are quite different from the previous simulation. But the main significant difference is that here γ_t is larger than γ_d . This has the following consequence, as is visible in Figure 12 which shows a terrace generation: the water which is contained in agar is used more. Apart from this difference, the way a terrace is created is very similar to simulation 1.

The first picture shows the situation at a moment when swarmer cells are de-differentiating and producing vegetative cells which are growing by cellular division. This is drying the extra cellular matrix.

The second picture shows a colony thickness, near the colony edge, larger than 1. Then thickness increases thanks to elongating cells which are turning into swarmer cells. The extra cellular matrix near the colony edge is dry, while towards the colony center it is wet.

The third picture shows the situation at the beginning of the consolidation phase. At this moment, the extra cellular matrix near the colony edge and in the colony center is wet. Between the

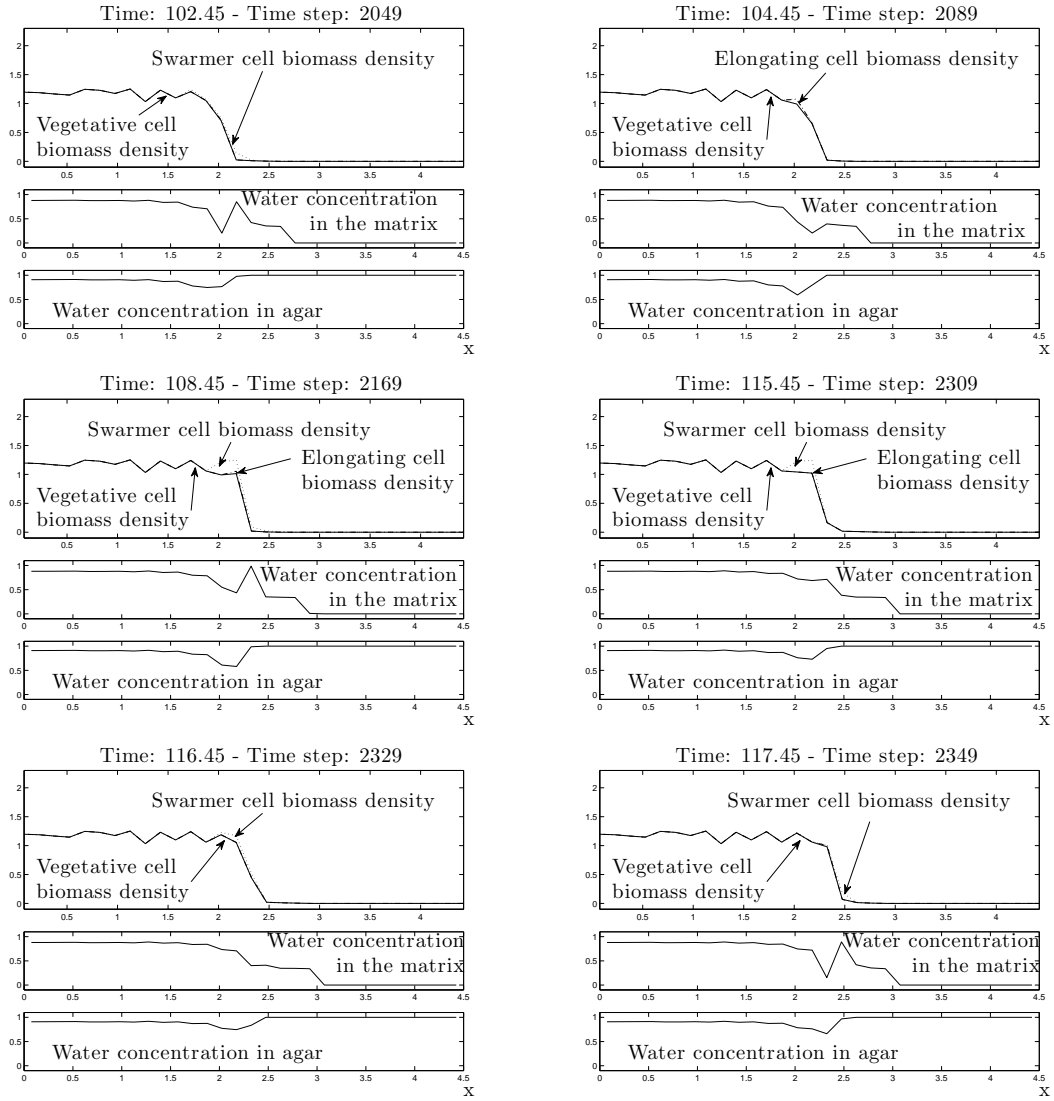


Figure 12: *Simulation 3 - Generation of a terrace.*

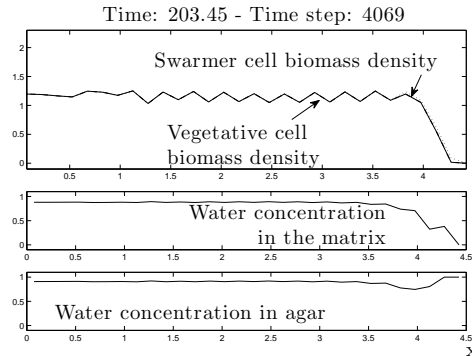


Figure 13: *Simulation 3 - End of the colonization.*

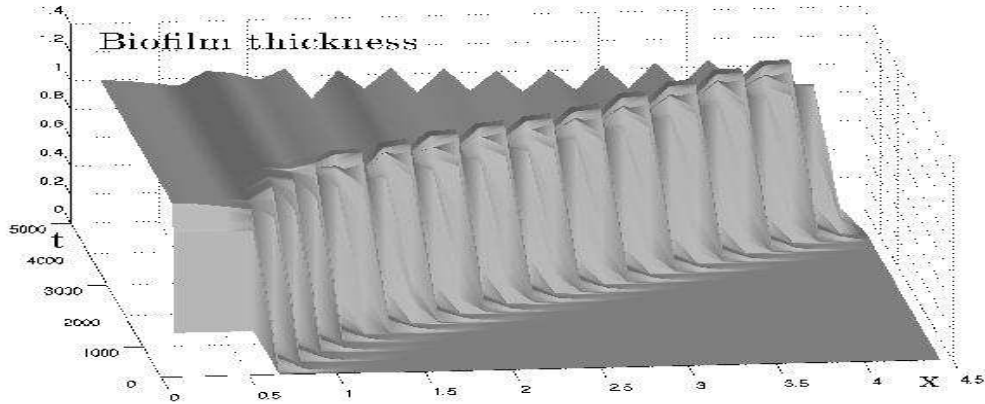


Figure 14: *Simulation 3 - Summarize of the swarm phenomenon.*

colony edge and the the colony center the water concentration of the extra cellular matrix increases.

The swarm colony shape does not evolve much until the moment of the third picture but the extra cellular matrix water concentration increases.

The fifth picture shows the moment when the de-differentiation begins which will soon lead to the situation in the sixth picture.

The situation in the sixth picture is similar to the one in the first picture but with a colony edge which has moved towards the right.

Figure 13 shows the situation at the end of the colonization. Here again, as in Figures 14 and 15 we may observe the relative regularity of the terraces.

6 Conclusion

In this paper, we add a bio-physical slant in the *Proteus mirabilis* swarm description. The scientific method we use for this is as follows. We first express the bio-physical principles on which, according to us, the swarm phenomenon could be based. Then, we translate those principles into a model which is implemented. Simulations show that the model behaviour may recover many of the aspects observed *in situ* and listed in the introduction. This leads to the conclusion that the previously expressed bio-physical principles are certainly the right ones to contribute to a swarm explanation.

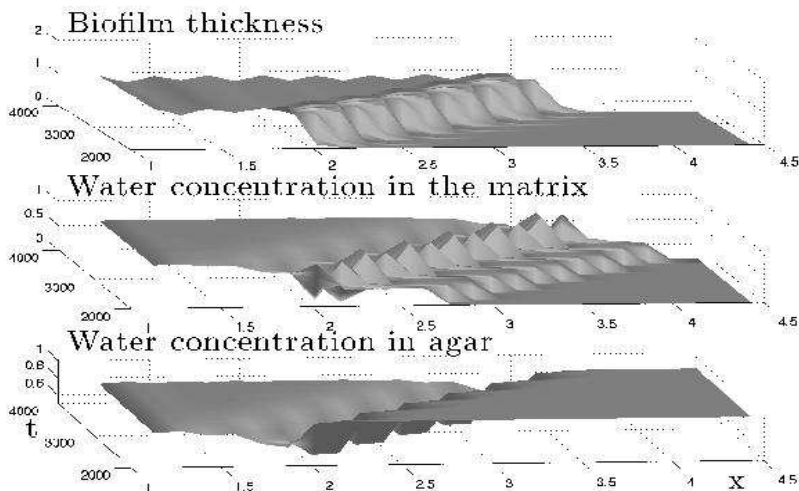


Figure 15: *Simulation 3 - Visualization of the relative positions of terraces, matrix water concentration maxima and agar water concentration minima.*

Or, more modestly, those bio-physical principles are first way-marks on the path leading to a bio-physical understanding of the swarm phenomenon.

However, many questions need to be tackled. From the modelling point of view, we notice that the model built here is dimensionless. This means that variables have no physical unit and that fields are of magnitude order 1. Therefore, even if the model built here can qualitatively recover the swarm phenomenon, we are far from a model which can give quantitative results. In order to build a model for quantitative simulations, we need to take into account the physical magnitudes of the phenomenon and to analyze physical constant ratios.

From the mathematical point of view, it would be nice to set out an existence result for the solution of the model built here. Moreover, we may notice that this model is unstable. In particular, it has been difficult to find values of the parameters that have led to simulations showing terraces. The stability properties, with respect to terrace generation or to short-term evolution or to long-term behaviour of the model is certainly a very interesting topic which may bring out biological answers.

From the numerical point of view, the organic assumption concerning age and time steps: $\Delta b = \Delta a = \Delta t$, which is needed to make the numerical scheme to be biomass preserving, will certainly result in bad computational results if the present method is applied for operational simulations. Indeed, the simulation of a real *Proteus mirabilis* swarm experiment requires a time step which is much smaller than the ageing characteristic time to resolve the dynamics in space. Hence, it is important to find ways to reduce the induced cost.

The first way that can be considered, consists in noticing that the biomass preservation property is always realised if the ageing process is done only every ν time steps, for an integer ν , setting $\Delta b = \Delta a = \nu \Delta t$ and modifying the method in the following way. Initializing formula (4.1), (4.4), (4.8) and (4.20) are left unchanged.

Then for values of $n \in \nu \mathbb{N}^*$, formula (4.2) is applied removing term \mathcal{D}_i^n and replacing Δt by $\nu \Delta t$ and formula (4.5) is applied replacing Δt by $\nu \Delta t$. Formula (4.6) to (4.19) and (4.21) to (4.23) are applied in state.

For values of $n \notin \nu \mathbb{N}$, formula (4.2) is replaced by

$$Q_i^{n+1} = Q_i^n + \mathcal{D}_i^n \text{ if } n \in (\nu \mathbb{N}^* + 1) \text{ and } Q_i^{n+1} = Q_i^n \text{ otherwise ,} \quad (6.1)$$

formula (4.5) is not applied, formula (4.6) and (4.7) are replaced by

$$\zeta_{k,i}^{n+1} = \zeta_{k,i}^n \text{ for every } i \text{ and every } k, \quad (6.2)$$

transfer condition (4.9) is not applied, (4.10) is replaced by

$$\rho_{k,p,i}^{n+1/2} = \rho_{k,p,i}^n, \quad (6.3)$$

and (4.13) and (4.14) are replaced by

$$\rho_{k,p,i}^{n+1} = \rho_{k,p,i}^{n+1/2} + \frac{\Delta t}{\Delta x} (F_{k,p,i-1/2}^n - F_{k,p,i+1/2}^n), \text{ for every } p \text{ and } k, \quad (6.4)$$

with fluxes given by (4.12) and (4.11). The definitions (4.16) to (4.18) remain the same (but we can notice that \mathcal{M}_i^n do not evolve). Finally (4.19), (4.21), (4.22) and (4.23) are applied in state.

The second way that needs to be investigated, consists in following the method set out in Ayati [1] and which consists in deducing from equations (3.3) and (3.9) evolution equations for functions $\zeta(t, a + t, x)$ and $\rho(t, a + t, b + t, x)$. From those equations we will be able to build age discrete equations involving age discretization possibly time dependant and not requiring an organic link between time and age steps.

From the biological point of view, it would be of great interest to enrich the model in order to take into account genetic or chemical events. In particular, it would be nice to understand how gene expressions may regularize terrace generation.

References

- [1] B. P Ayati. A variable time step method for an age-dependent population model with nonlinear diffusion. *SIAM J. Numer. Anal.*, 37:1571–1589, 2000.
- [2] B. P Ayati. A structured-population model of *Proteus mirabilis* swarm-colony development. *J. Math. Biol.*, 52:93–114, 2006.
- [3] B. P Ayati. Modeling the role of the cell cycle in regulating *Proteus mirabilis* swarm-colony development. *Appl. Math. Lett.*, 20:913–918, 2007.
- [4] B. P Ayati. A comparison of the dynamics of the structured cell population in virtual and experimental *Proteus mirabilis* swarm colonies. *Appl. Num. Math.*, to appear.
- [5] B. P. Ayati and T. F. Dupont. Galerkin methods in age and space for a population model with nonlinear diffusion. *SIAM J. Numer. Anal.*, 40:1064–1076, 2002.
- [6] B. P. Ayati and I. Klapper. A multiscale model of biofilm as a senescence-structured fluid. *Multiscale Model. Simul.*, 6:347–365, 2007.
- [7] Belas B. *Proteus mirabilis* and other swarming bacteria. In A. Shapiro and M. Dworkin, editors, *Bacteria as Multicellular Organisms*, chapter 2, pages 183–219. Oxford University Press, 1997.
- [8] E. Ben-Jacob and I. Cohen. Cooperative formation of bacterial patterns. In A. Shapiro and M. Dworkin, editors, *Bacteria as Multicellular Organisms*, chapter 14, pages 394–416. Oxford University Press, 1997.
- [9] H.C. Berg. Swarming motility: it better be wet. *Curr. Biol*, 15:R599–600, 2005.
- [10] E. O. Budrene and H. C. Berg. Complex patterns formed by motile cells of *Escherichia coli*. *Nature*, 349:630–633, 1991.

- [11] B.G. Chen, L. Turner, and H.C. Berg. The wetting agent required for swarming in *Salmonella enterica* serovar typhimurium is not a surfactant. *J. Bact.*, 189:8750–8753, 2007.
- [12] M. Dworkin. Multiculturalism versus the single microbe. In A. Shapiro and M. Dworkin, editors, *Bacteria as Multicellular Organisms*, chapter 1, pages 3–13. Oxford University Press, 1997.
- [13] S. E. Esipov and J. A. Shapiro. Kinetic model of *proteus mirabilis* swarm colony development. *J. Math. Biol.*, 36:249–268, 1998.
- [14] K.J. Falconer. *Fractal geometry. Mathematical foundations and applications*. John Wiley and sons, Ithaca, New York, 1990.
- [15] J.O Falkinham and P.S. Hoffman. Unique developmental characteristics of the swarm and short cells of *Proteus vulgaris* and *Proteus mirabilis*. *J. Bact.*, 158:1037–1040, 1984.
- [16] E. Frénod. Existence result of a model of *Proteus mirabilis* swarm. *Diff. Integr. Equations*, 19(6):697–720, 2006.
- [17] M. Gué, V. Dupont, A. Dufour, and O. Sire. Bacterial swarming: A biological time-resolved FTIR-ATR study of *proteus mirabilis* swarm-cell differentiation. *Biochemistry*, 40:11938–11945, 2001.
- [18] M. E. Gurtin. A system of equations for age-dependent population diffusion. *J. Theor. Biol*, 40:389–392, 1973.
- [19] M. E. Gurtin and R. C. Mac Camy. Non-linear age-dependent population dynamics. *Arch. Rat. Mech. Anal.*, 54:281–300, 1974.
- [20] G Hauser. *Über Fäulnisbakterien und deren Beziehung zur Septicämie*. FGW Vogel, Leipzig, Germany, 1885.
- [21] J.F. Hoeniger. Cellular changes accompanying the swarming of *Proteus mirabilis*. I. Observations of living cultures. *Can. J. Microbiol.*, 10:1–9, 1964.
- [22] S.A. Kaufmann. *The Origins of Order, Self-Organization, and Selection in Evolution*. Oxford University Press, New York, 1993.
- [23] J. Keirsse, E. Lahaye, A. Bouter, V. Dupont, C. Boussard-Plédel, B. Bureau, J.-L. Adam, V. Monbet, and O. Sire. Mapping bacterial surface population physiology in real-time: Infrared spectroscopy of *Proteus mirabilis* swarm colonies. *Appl. Spectrosc.*, 60:584–591, 2006.
- [24] E. Lahaye, T. Aubry, N. Kervarec, P. Douzenel, and O. Sire. Does water activity rule *P. mirabilis* periodic swarming? I. Biochemical and functional properties of the extracellular matrix. *Biomacromolecules*, 8:1218–1227, 2007.
- [25] E. Lahaye, T. Aubry, V. Fleury, and O. Sire. Does water activity rule *P. mirabilis* periodic swarming? II. Viscoelasticity and water balance during swarming. *Biomacromolecules*, 8:1228–1235, 2007.
- [26] Ph. Laurençot and Ch. Walker. An age and spatially structured population model for *Proteus mirabilis* swarmcolony development. *Math. Model. Nat. Phenom*, to appear.
- [27] Ph. Laurençot and Ch. Walker. *Proteus mirabilis* swarm-colony development with drift. to appear.
- [28] R. J. LeVeque. *Numerical Methods for Conservation Laws*. Birkäuser, 1992.

- [29] R. J. LeVeque. *Finite Volume Methods for Hyperbolic Problems*. Cambridge University Press, 2002.
- [30] B.B. Mandelbrot. *The fractal Geometry of Nature*. Freeman, San Francisco, 1982.
- [31] J. E. Manos, Artimovich, and R. Belas. Enhanced motility of a proteus mirabilis strain expressing hybrid FlaAB flagella. *Microbiol.*, 150:1291–1299, 2004.
- [32] M. Matsushita. Formation of colony patterns by a bacterial cell population. In A. Shapiro and M. Dworkin, editors, *Bacteria as Multicellular Organisms*, chapter 13, pages 366–393. Oxford University Press, 1997.
- [33] T. Matsuyama, Y. Takagi, Y. Nakagawa, H. Itoh, and J. and Matsuyama M. Wakita. Dynamic aspects of the structured cell population in a swarming colony of *Proteus mirabilis*. *J. Bact.*, 182:385–393, 2000.
- [34] A. J. Mc Coy, H. Liu, T. J. Falla, and J. S. Gunn. Identification of *Proteus mirabilis* mutants with increased sensitivity to antimicrobial peptides. *Antimicrobial Agents and Chemotherapy*, 45:2030–2037, 2001.
- [35] G. E. Medvedev, T. J. Kapper, and Koppel N. A reaction-diffusion system with periodic front dynamics. *SIAM J. Appl. Math.*, 60:1601–1638, 2000.
- [36] N.H Mendelson, B. Salhi, and C Li. Physical and genetic consequences of multicellularity in *Bacillus subtilis*. In A. Shapiro and M. Dworkin, editors, *Bacteria as Multicellular Organisms*, chapter 12, pages 339–365. Oxford University Press, 1997.
- [37] J.D Murray. *Mathematical Biology (I and II)*, volume 17 and 18 of *Interdisciplinary Applied Mathematics*. Springer, 2004.
- [38] O. Rauprich, M. Matsuchita, C. J. Weijer, F. Siegert, S. E. Esipov, and J. A. Shapiro. Periodic phenomena in *proteus mirabilis* swarm colony development. *J. Bact.*, 178:6525–6538, 1996.
- [39] R. Schneider, C.V. Lockatell, D. Johnson, and R. Belas. Detection and mutation of a luxS-encoded autoinducer in *Proteus mirabilis*. *Microbiol.*, 148:773–782, 2002.
- [40] J.A. Shapiro. Intercellular communication and genetic change in bacteria. In H.O. Halvorson, D. Pramer, and M. Rogul, editors, *Engineered Organisms in the Environment*, Scientific Issues, pages 63–69. American Society for Microbiology, 1985.
- [41] J.A. Shapiro. Mechanisms of DNA reorganization in bacteria. *Int. Rev. Cytol.*, 93:25–56, 1985.
- [42] J.A. Shapiro. Photographing bacterial colonies. *A.S.M. News*, 51:62–69, 1985.
- [43] J.A. Shapiro. Scanning electron microscope study of *Pseudomonas putida* colonies. *J. Bact.*, 164:1171–1181, 1985.
- [44] J.A. Shapiro. Organization of developing *E. coli* colonies viewed by scanning electron microscopy. *J. Bact.*, 197:142–146, 1987.
- [45] J.A. Shapiro. Bacteria as multicellular organisms. *Scientific American*, 256:82–89, 1988.
- [46] J.A. Shapiro. Natural genetic engineering of the bacterial genome. *Curr. Opin. Genet. Devel.*, 3:845–848, 1993.
- [47] J.A. Shapiro. Pattern and control in bacterial colonies. *Science Progress*, 76:399–424, 1994.

- [48] J.A. Shapiro. Multicellularity: The rule, not the exception. In A. Shapiro and M. Dworkin, editors, *Bacteria as Multicellular Organisms*, chapter 2, pages 14–49. Oxford University Press, 1997.
- [49] J.A. Shapiro and M. Dworkin, editors. *Bacteria as Multicellular Organisms*. Oxford University Press, 1997.
- [50] Stickler. Susceptibility of antibiotic-resistant gram-negative bacteria to biocides: a perspective from the study of catheter biofilms. *J. Appl. Microbiol.*, 92:163S–170S, 2002.
- [51] R. Thom. *Stabilité structurelle et morphogénèse*. InterEditions, Paris, 1977.